

# Characteristics of Transient Behavior of Gas Flow in Microchannels

M. Ashhab\*<sup>a</sup> A. Muhtaseb<sup>b</sup>

<sup>a</sup>Department of Mechanical Engineering, The Hashemite University, Zarqa, 13115, Jordan

<sup>b</sup>Mechanical Engineering Department, University of Jordan, Amman, 11942, Jordan

## Abstract

In this paper, a three-dimensional numerical model of transient incompressible gaseous flow in microchannels was established. The influence of changing the inlet velocity on the transient fluid flow is analyzed – using finite volume software (Fluent 6.3). The study showed that the transient period is decreased when the inlet velocity is increased, the maximum velocity is almost twice the entrance velocity, and the pressure has a small variation in the entrance of the channel and after that it becomes constant. It was concluded that despite of the fact that the transient behavior in micro systems is usually neglected due to its quick response, the transient terms of the Navier Stokes equations should be taken into consideration when dealing with flow behaviors that may occur in micro or nano seconds.

© 2011 Jordan Journal of Mechanical and Industrial Engineering. All rights reserved

**Keywords:** Microchannels; Gas Flow; Navier Stokes; Transient Response

## Nomenclature

Dh	hydraulic diameter (lm)
h	channel height (lm)
T	temperature (K)
t	Time (Second)
a	tangential momentum accommodation coefficient
l	dynamic viscosity (N/m <sup>2</sup> s)
Re	Reynolds number
c	specific heat ratio (J/(kg K))
Kn	Knudsen number
leff	modified dynamic viscosity (N/m <sup>2</sup> s)
c	specific heat ratio
P	pressure (Pa)
f	Dancy friction factor
u v	x y z-axes velocity (m/s)
w	averaged velocity (m/s)
U	density (kg/m <sup>3</sup> )
q	centerline velocity (m/s)
Uc	slip velocity (m/s)
Us	wall velocity (m/s)
Uw	mean free path (lm)
k	

## Subscripts

w	wall
in	inlet
out	outlet

## 1. Introduction

Microchannels are considered the very elementary structure of all micro and/or nano systems that include the process of fluid flow. Several researchers studied the microchannels and found out that the both flow and heat characteristics differ from that in the classical systems; these different characteristics are detailed in the paper of Mohamed GH in 1999 [1].

Rarefaction, viscosity heating, surface roughness and compressibility significantly affect the flow and heat characteristics in the gaseous flow; either of these issues are considered separately or simultaneously [2]. In reference to Knudsen number Kn, Beskok and Karniadakis [3] classified the gas flow in microchannels into four flow regimes: continuum flow regime ( $Kn < 0.001$ ) at which the compressibility plays a key role, slip flow regime ( $0.001 < Kn < 0.1$ ), transition flow regime ( $0.1 < Kn < 10$ ) and free molecular flow regime ( $Kn > 10$ ).

The effect of microchannels in continuum region was studied by Asako et al [4,5] without handling the effect of rarefaction where it is found that both friction factor and Reynolds number in quasi-fully developed region are functions of Mach number; and they set these correlations there. Numerical analysis of fully developed laminar slip flow and heat transfer in trapezoidal microchannels had

\* Corresponding author. e-mail: sami@hu.edu.jo

been studied by Bin et al. [6] with uniform wall heat flux boundary conditions. In their investigation, the compressibility effect was neglected. The influences of velocity slip and temperature jump on friction coefficient and Nusselt number were investigated in detail. Orhan and Mete [7] analyzed laminar forced convective heat transfer of a Newtonian fluid in a micropipe where they took into account the viscous dissipation effect, the velocity slip and the temperature jump at the wall.

Wei et al. [8] investigated the steady-state convective heat transfer for laminar, two-dimensional, incompressible rarefied gas flow by the finite-volume finite difference scheme with slip flow and temperature jump conditions. Several boundary conditions were considered, and flow and heat transfer characteristics were studied systemically. Nishanth et al. [9] provided solution of the Navier-Stokes equations for gaseous slip flow in long microchannels with a second-order accurate slip boundary condition at the walls.

The compressibility effect had been taken into account in their analysis, which is usually neglected. They pointed out that the compressibility effect can not be neglected in rarefaction flow. Recently, T.T. Zhang [2] performed a study of compressibility effect combined with rarefaction effect on local friction factor in slip region.

It was noted that there is no study made previously on the transient fluid behavior in microchannels, due to the fact that most of the used applications occur in a relatively large time scale. But what if we are dealing with a very rapid system that deals with nanoseconds for example! Towards this end work had handled here showing some of the air behaviors in microchannels and analyzing the fluid flow in the transient region.

## 2. Model Setup

The work in this research intends to investigate the transient hydrodynamics behavior of fluid flow in microchannels by adopting the continuum approach but with no-slip flow boundary conditions. In order to verify the validity of the continuum approach with no-slip flow boundary conditions we refer to the Knudsen number which is defined as the mean free path for the particle dynamics divided by the hydraulic diameter of the microchannel. The Knudsen number must have a value less than 0.001 for our approach to be valid. The mean free path for the particle dynamics in the atmosphere, and assuming standard temperature and pressure, i.e. 25 °C and 1 atm, is  $\lambda \approx 8 \times 10^{-10}$  m, or approximately  $2.6 \times 10^{-9}$  ft. The hydraulic diameter of the channel used is  $20 \times 10^{-6}$  m. Therefore, the Knudsen number is equal to  $4 \times 10^{-5}$  which is less than 0.001 and consequently Navier Stokes equation with no-slip conditions shall be used.

In this paper, a square-cross sectional microchannel is analyzed, as shown in Fig. 1. The length of channel is  $L$  and the hydraulic diameter is  $D_h = \frac{4 \times \text{cross-sectional area}}{\text{perimeter}}$ . In our case,  $D_h$  equals

the height of the square.

The simulations are performed based on the following assumptions:

- The governing equations based on Navier-Stokes equations with no-slip boundary can be used to describe the physical processes.

- The flow is laminar (very small Re number, in our case the maximum Re = 137.5).
- Incompressible fluid ( $Ma \leq 0.3$ )
- The body forces and the effect of viscosity heating are neglected.
- The heat transfer is not considered in the calculation.

The resulting governing equations are

Continuity equation:

$$\frac{\partial \rho}{\partial t} + \frac{\partial \rho u}{\partial x} + \frac{\partial \rho v}{\partial y} + \frac{\partial \rho w}{\partial z} = 0$$

Momentum equations:

$$\rho \frac{Du}{Dt} = \left( -\frac{\partial(p)}{\partial x} \right) + \mu_{\text{eff}} \left( \frac{\partial^2 u}{\partial x^2} + \frac{\partial^2 u}{\partial y^2} + \frac{\partial^2 u}{\partial z^2} \right) + \frac{\mu_{\text{eff}}}{3} \frac{\partial}{\partial x} \left( \frac{\partial u}{\partial x} + \frac{\partial v}{\partial y} + \frac{\partial w}{\partial z} \right)$$

$$\rho \frac{Dv}{Dt} = \left( -\frac{\partial(p)}{\partial y} \right) + \mu_{\text{eff}} \left( \frac{\partial^2 v}{\partial x^2} + \frac{\partial^2 v}{\partial y^2} + \frac{\partial^2 v}{\partial z^2} \right) + \frac{\mu_{\text{eff}}}{3} \frac{\partial}{\partial x} \left( \frac{\partial u}{\partial x} + \frac{\partial v}{\partial y} + \frac{\partial w}{\partial z} \right)$$

$$\rho \frac{Dw}{Dt} = \left( -\frac{\partial(p)}{\partial z} \right) + \mu_{\text{eff}} \left( \frac{\partial^2 w}{\partial x^2} + \frac{\partial^2 w}{\partial y^2} + \frac{\partial^2 w}{\partial z^2} \right) + \frac{\mu_{\text{eff}}}{3} \frac{\partial}{\partial x} \left( \frac{\partial u}{\partial x} + \frac{\partial v}{\partial y} + \frac{\partial w}{\partial z} \right)$$

Ideal gas law:

$$P = \rho RT$$

Variation in diffusion coefficient  $\mu_{\text{eff}}$  is given by:

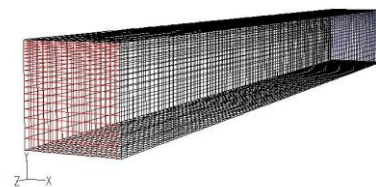
$$\mu_{\text{eff}} = \frac{\mu}{(1 + Kn)}$$

The boundary conditions of the above described problem are expressed as follows

On the wall:  $y = \pm 0.5h \rightarrow U_w = 0.0$ .

At the inlet:  $x = 0.0 \rightarrow U = \text{Constant}$  (different three inlet velocities are considered).

At the outlet:  $x = L, P = P_{\text{out}}$ .



Grid  
May 12, 2009  
FLUENT 6.3 (3d, pbns, lam)

Figure 1: Meshed 3-dimensional microchannel used for analysis.

### 3. Numerical Method

The governing equations with boundary conditions as described in the previous section were solved by the CFD code, CFX-ACE. The equations were discretized by means of a fully implicit second-order finite-volume approach with second-order upwind advection scheme. In this work, the grid points used in the x, y, and z directions were selected to be 20, 20 and 200 respectively as this channel size achieves the best performance [2].

Fluent (finite volume method based software) is used to get the results. The numerical solution is obtained by an explicit iteration procedure and the solution converges when the maximum residuals of continuity equation was less than  $10^{-10}$ .

### 4. Results and Discussion

#### 4.1. Velocity distribution with time:

The center line velocity distribution versus the time are presented in Figs 2, 3, 4 and 5 for the case of  $D_h = 20 \mu\text{m}$ , inlet velocities of 0.1, 1.0 and 10 m/s respectively and for incompressible flow. Note that the center line velocities increase with time. The time needed for the transient period shrinks as the inlet velocity increases.

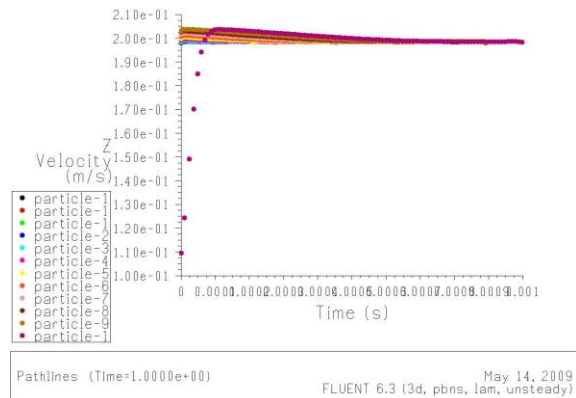


Figure 2: Velocity magnitude versus time at the centerline of the microchannel when the inlet velocity is 0.1m/sec.

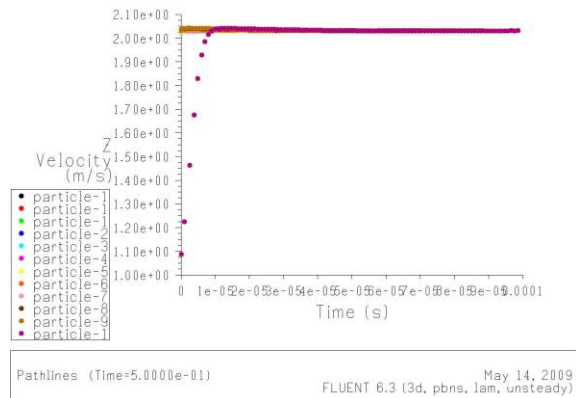


Figure 3: Velocity magnitude versus time at the centerline of the microchannel when the inlet velocity is 1.0m/sec.

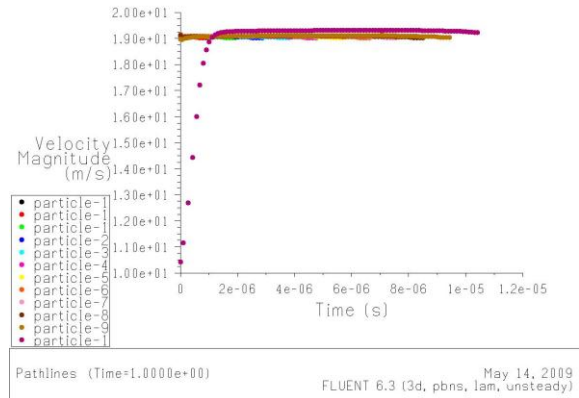


Figure 4: Velocity magnitude versus time at the centerline of the microchannel when the inlet velocity is 10 m/sec.

#### 4.2. Velocity distribution along the Microchannel:

The variation of the velocity along the channel for the three above mentioned velocities is shown in Figs 5, 6 and 7 respectively at which the velocity vectors are displayed.

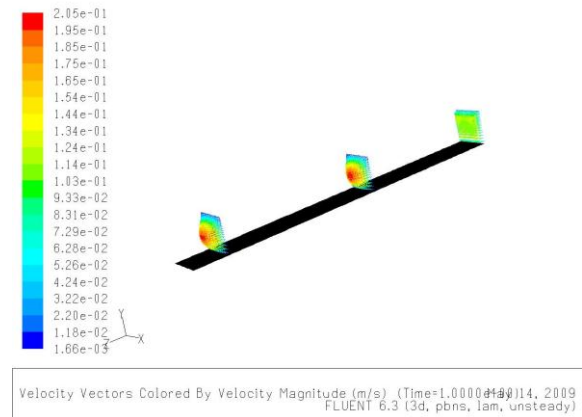


Figure 5: Velocity vectors along the microchannel when the inlet velocity is 0.1 m/sec.

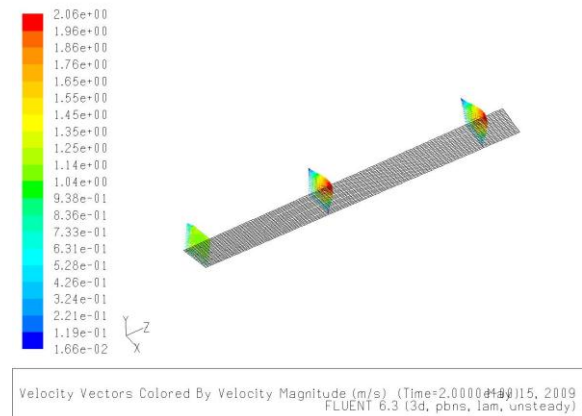


Figure 6: Velocity vector along the microchannel when the inlet velocity is 1.0 m/sec.

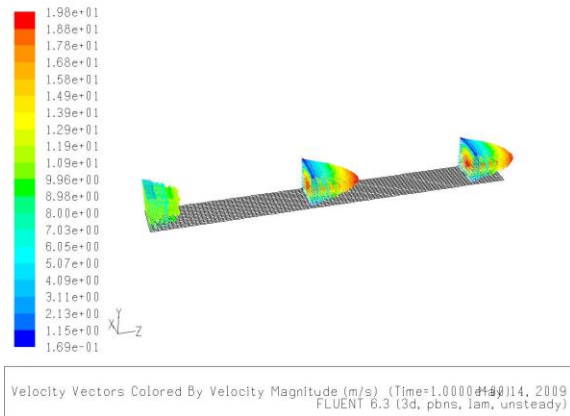


Figure 7: Velocity vector along the microchannel when the inlet velocity is 10m/sec.

From all of the above figures it is clear that all the percentage of the maximum velocity over the inlet velocity is almost constant with an average factor of 2.03, that is  $U_{max} = 2.03 \times U_{in}$ . This implies that the maximum velocity is twice the entrance velocity in the transient region.

4.3. Pressure distribution along the Microchannel:

From the pressure contours shown in Figs 8, 9 and 10, it is clear that the upstream pressure can have small variation from one point to another at the same cross-section. Going a small distance to the downstream direction, it is clear that the pressure becomes constant across the same cross section.

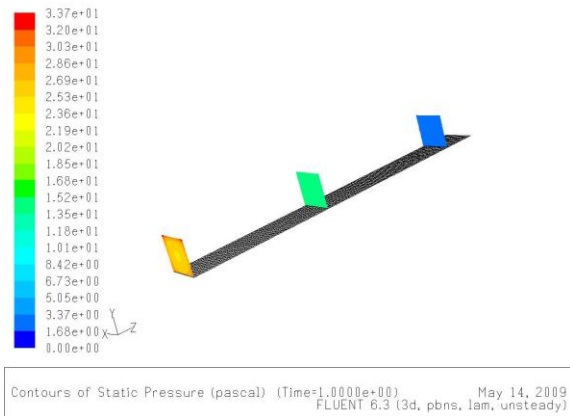


Figure 8: Pressure contours along the microchannel when the inlet velocity is 0.1m/sec.

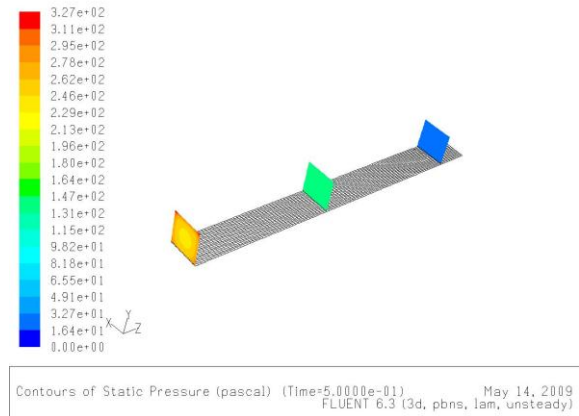


Figure 9: Pressure contours along the microchannel when the inlet velocity is 1.0m/sec.

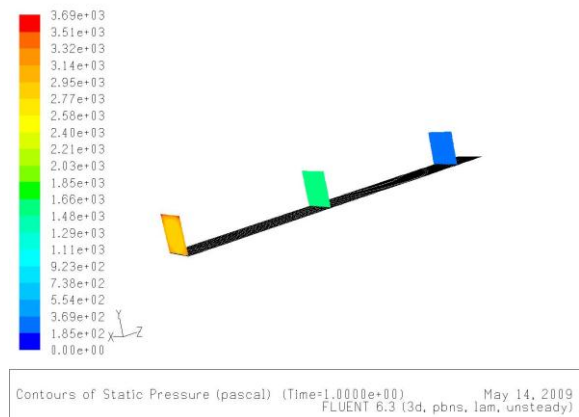


Figure 10: pressure contours along the microchannel when the inlet velocity is 10m/sec.

It can be clearly noted from Figs 7,8 and 9 that the maximum pressure occurs at the walls of the channel at the inlet, where also and the maximum inlet velocity and the maximum wall pressure occur. The relationship of the maximum pressure with the inlet velocity is linear while fixing the cross-sectional area and is found as

$$P_{max} = 373.7U_{in} - 46.7$$

The maximum pressure in the microchannel is important since the fluid particles could be pressure sensitive and may be destroyed if exposed to high values of pressure.

5. Conclusion

Although the transient behavior of fluids in microchannels was not a spot of concern to many researchers before, the transient behavior and transient terms of Navier-Stokes equations shall be taken in consideration when dealing with applications that occur in a micro and/or nanoseconds. Both of the maximum channel velocity and the maximum channel pressure have linear relationships with the inlet velocity which was proven and derived in this work based on numerical solution and computer simulation.

## References

- [1] GH. Mohamed "The fluid mechanics of microdevices". *J Fluid Eng*, Vol. 121, 1999, 5-33.
- [2] T.T. Zhang, L. Jai, Z.C. Wang, C.W. Li. "Slip flow characteristics of compressible gaseous in microchannels", *Energy Conversion and Management* 2009.doi:10.1016/j.enconman.2009.03.032.
- [3] A. Beskok , GE. Karniadakis "Simulation of heat and momentum transfer in complex micro-geometries". *J Thermophys Heat Transfer* Vol. 8, 1994, 355-70.
- [4] Y. Asako, K Nakayama, T. Shinozuka "Effect of compressibility on gaseous flows in a micro-tube". *Int J Heat Mass Transfer* Vol. 48, 2005, 4985-94.
- [5] Y. Asako, T Pi, ET Stephen, FY Mohammad. "Effect of compressibility on gaseous flows in micro-channels". *Int J Heat Mass Transfer* Vol. 46, 2003, 3041-50.
- [6] C. Bin, W.C. Guang, Y. Quan, "Fully developed laminar flow and heat transfer in smooth trapezoidal microchannel". *Int Commun Heat Mass* Vol. 32, 2005, 1211-20.
- [7] Orhan A, Mete A. "Heat and fluid flow characteristics of gases in micropipes". *Int. J Heat Mass Transfer* Vol. 49, 2006,1723-30.
- [8] S. Wei , K. Sadik , G. Yazicioglu Almila "A numerical study of single-phase convective heat transfer in microtubes for slip flow". *Int J Therm Sci* Vol. 46, 2007, 1084-94.
- [9] D . Nishanth, A . Abhishek, A . Amit. "Analytical solution of gaseous slip flow in long microchannels". *Int J Heat Mass Transfer* Vol. 50, 2007, 3411-21.